Available online at www.sciencedirect.com
ScienceDirect
Trans. Nonferrous Met. Soc. China 24(2014) 184−191
Transactions of Nonferrous Metals Society of China
www.tnmsc.cn

Effect of Sb content on properties of Sn−Bi solders

Cheng ZHANG[1], Si-dong LIU[1], Guo-tong QIAN[2], Jian ZHOU[1], Feng XUE[1]

1. School of Materials Science and Engineering, Southeast University, Nanjing 211189, China;
2. Shaoxing Tianlong Tin Materials Co., Ltd., Shaoxing 312001, China

Received 19 December 2012; accepted 15 July 2013

Abstract: The effect of Sb content on the properties of Sn−Bi solders was studied. The nonequilibrium melting behaviors of a series of Sn−Bi−Sb solders were examined by differential scanning calorimetry (DSC). The spreading test was carried out to characterize the wettability of Sn−Bi−Sb solders on Cu substrate. The mechanical properties of the solders/Cu joints were evaluated. The results show that the ternary alloy solders contain eutectic structure resulting from quasi-peritetic reaction. With the increase of Sb content, the amount of the eutectic structure increases. At a heating rate of 5 °C/min, Sn−Bi−Sb alloys exhibit a higher melting point and a wider melting range. A small amount of Sb has an impact on the wettability of Sn−Bi solders. The reaction layers form during spreading process. Sb is detected in the reaction layer while Bi is not detected. The total thickness of reaction layer between solder and Cu increases with the increase of the Sb content. The shear strength of the Sn−Bi−Sb solders increases as the Sb content increases.

Key words: lead-free solder; Sn−Bi−Sb alloy; microstructure; melting behavior; wettability

1 Introduction

Solder material plays a crucial role in providing the necessary electrical and mechanical interconnections in an electronic assembly. Sn−Pb solders have been widely used throughout the electronic packaging industries. However, mounting healthy and environmental concerns over the toxicity of Pb present in these alloys have led to the banning of its use in electronics manufacturing by USA, Japan, and European Union [1−4]. As a consequence, the study on lead-free solders attracts more and more world-wide attention. In many cases, components that are sensitive to temperature [5,6] need to be soldered at or below 200 °C. It brings the low temperature soldering issue. The eutectic temperature of Sn−Bi binary alloys is 138 °C, which obviously meets the temperature requirement of low-temperature soldering [7]. The low melting point gives the alloy an advantage in outer packaging [8]. However, the segregation of impurities always seriously deteriorates physical and mechanical properties of the material, so does Bi segregation [9]. The wettability of Sn−58Bi is poorer than that of Sn−Pb solders [10,11]. ZHU et al [12] tried to employ electrodeposition of Ag thin film onto the Cu substrate to successfully prevent the interfacial embrittlement of SnBi/Cu interconnects even after a long time aging. LI et al [13] studied the effect of rapid cooling on the properties of Sn−20Bi−X alloys. MANASIJEVIC et al [14] studied the phase equilibrium and thermodynamics of Sn−Bi−Sb system. In this work, a small amount of Sb was added in Sn−Bi solders while the content of Bi decreased. One attempts to reduce the adverse effect of Bi in Sn−Bi solder by lowering its content, while maintaining the wettability.

2 Experimental

The Sn−Bi−Sb alloys were prepared from pure Sn and Bi (both 99.95%, mass fraction) and pure Sb(99.5%, mass fraction). Sb was added in the form of Sn−Sb intermediate alloys. Required quantities of alloys were melted in a pit furnace under a nitrogen atmosphere. After the Sn−Sb alloys were molten and cooled for a while, the melt was thoroughly agitated and the dross was erased. Then, Bi particles were added into the molten Sn and Sn−Sb intermediate alloys at 280 °C in a crucible. The melt was agitated to effect homogenization.

Foundation item: Project (51004039) supported by the National Natural Science Foundation of China; Project (2012713) supported by the Cooperation Promoting Foundation in Science and Technology of Shaoxing City, China
Corresponding author: Jian ZHOU; Tel/Fax: +86-25-52090689; E-mail: jethro@seu.edu.cn
DOI: 10.1016/S1003-6326(14)63046-6

The casting was done in air. The designated compositions were considered the actual ones.

The microstructures of the specimens were analyzed by scanning electron microscopy (SEM) and optical microscopy. The fracture morphologies of solder/Cu joints were analyzed by SEM. The compositional profiles near the interface were analyzed by energy dispersive X-ray diffraction (EDX). Phase identification was carried out using an X-ray diffractometer operated at 40 kV, and Cu K_α radiation was used, with diffraction angle 2θ from 10° to 90° and a scanning speed of 2 (°)/min. The differential scanning calorimetry (DSC) was carried out in a NETZSCH simultaneous DSC−TG at a heating rate of 5 K/min. The test was operated within the range of room temperature (RT) to 200 °C.

The spreading test was carried out to evaluate the wettability of Sn−Bi−Sb solders on Cu substrate. The Cu sheets (5 mm×5 mm×0.1 mm) were treated in an aqueous solution of 1% HCl (volume fraction) and then an aqueous solution of 0.3% NaOH (volume fraction), followed by ultrasonically cleaning in ethanol. The spreading ratio (S_R) was calculated as follows:

$$S_R = \frac{D-H}{D} \times 100\% \quad (1)$$

where H stands for the height of solders after spreading; D stands for the diameter of solder balls. For one alloy, the average spreading ratio of at least three tests was used to measure its wettability on Cu substrate.

According to Japan industry standard JIS Z 3198−5 [15], the novel shear specimen (as shown in Fig. 1) was adopted to evaluate the mechanical properties of the solder joints with a CMT 4503 material testing machine. The shear speed was set as 2 mm/min. The Cu substrate had dimensions of 30 mm×5 mm×2 mm. The thickness between the two substrates was 0.3 mm. The substrate was put in the flux and dipped into the melting solders for 30 s. After soldering, a wedge was cut on each side of the joint. The gap between two wedges was 8 mm.

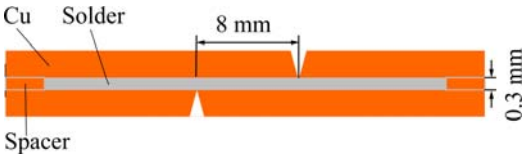

Fig. 1 Schematic illusion of shear strength tests for solder joints

3 Results and discussion

3.1 Structure

Figure 2 shows the microstructures of Sn−58Bi and Sn−Bi−Sb alloys. Sn−58Bi alloy shows the typical

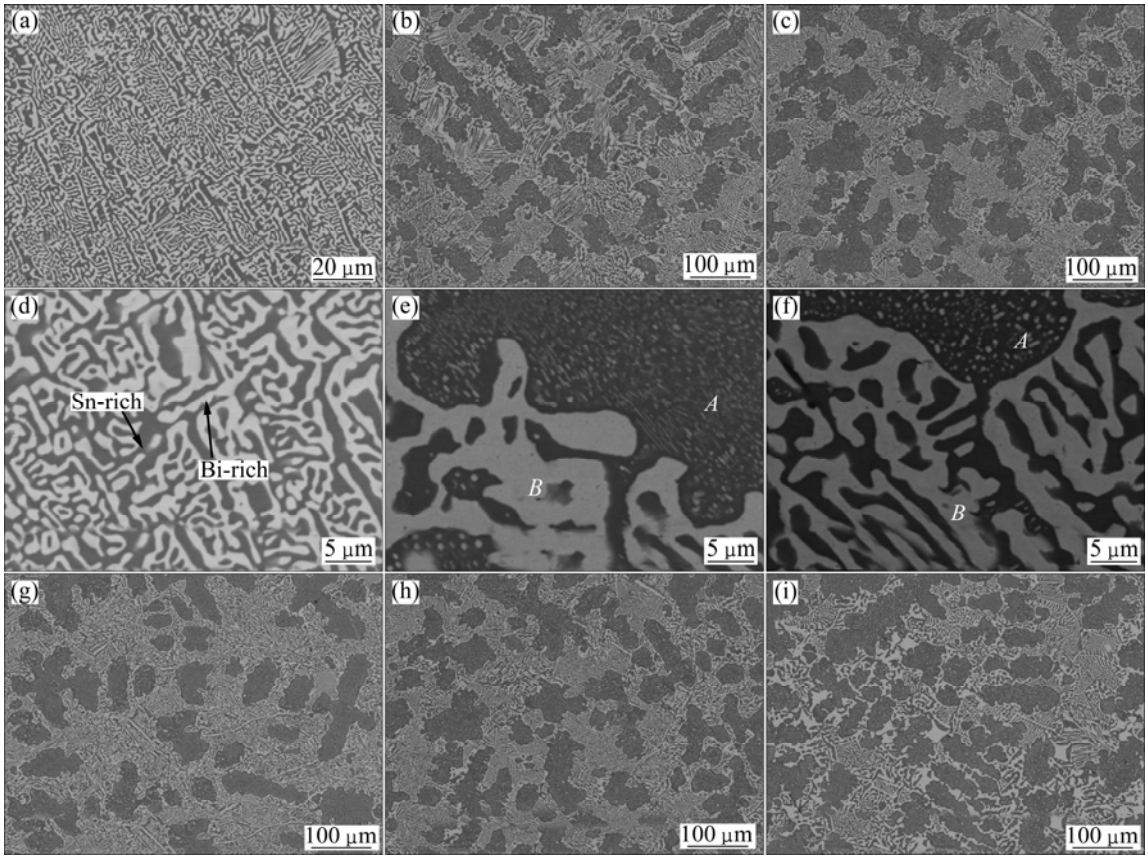

Fig. 2 SEM images of Sn−58Bi and Sn−Bi−Sb alloys: (a), (d) Sn−58Bi; (b), (e) Sn−52Bi−1.8Sb; (c), (f) Sn−48Bi−1.8Sb; (g) Sn−48Bi−1.4Sb; (h) Sn−48Bi−1.8Sb; (i) Sn−48Bi−2.4Sb

eutectic structure. The dark region is Sn phase and the white region represents Bi phase. For Sn−Bi−Sb alloys, two kinds of structures, i.e. Parts *A* and *B* are observed. Each part contains two phases, the dark phase and the light phase shown, respectively in the pictures (Figs. 2(e) and (f)).

Figure 3 and Table 1 show the EDX results of Sn−Bi−Sb alloy. It is seen that the dark phase is Sn phase and the light phase is Bi-rich phase. Previous thermodynamics studies [16,17] show that there are two reactions around the designed compositions. One is the eutectic reaction $L\rightarrow$(Sn)+(Bi). The other is the quarternary quasi-peritectic reaction $L+\beta\rightarrow$(Sn)+(Bi). Compared with the typical eutectic structure of Sn−58Bi, it can be concluded that part *A* in Figs. 2(e) and (f) is quasi-peritectic structure and part *B* in Figs. 2(e) and (f) is eutectic structure.

When Bi content changes, the proportion of each structure does not change much (Figs. 2(b), (c)). However, the proportion of quasi-peritectic structure increases as the Sb content increases (Figs. 2(g), (h), (i)). These are in agreement with results shown in the XRD patterns. Figure 4 shows the XRD patterns for different solders. For Sn−48Bi−*x*Sb alloys, the intensity of β phase increases when the Sb content increases. For Sn−*x*Bi−1.8Sb alloys, similar trend is not observed.

3.2 DSC

Figures 5 and 6 show the DSC profiles of nine Sn−Bi−Sb alloys. The temperatures of the endothermic peaks are shown in Table 2 and Table 3. Table 2 and Table 3 also give the melting ranges of these alloys derived from the DSC profiles. For Sn−Bi−Sb alloys, the melting behavior is different from that seen in eutectic alloy (Figs. 5 and 6). All the main peaks appear around 147 °C. The melting range of all Sn−Bi−Sb alloys is larger than that of the eutectic alloy. Second peaks are observed in many DSC profiles of Sn−Bi−Sb alloys. As the Bi content is reduced, the melting range becomes large obviously (Table 2). Meanwhile, when Sb content changes, the melting range and liquidus temperature reach the maximum around the Sn−48Bi−1.8Sb composition, and then starts to drop (Table 3). For melting range, it may be attributed to the fact that the proportion of eutectic structure will change when Bi or Sb content changes. For liquidus temperature, it is found that the primary phase changes to β phase when the Sb content is more than 1.8%. The second peaks imply that the remaining primary phases continue to melt after quasi-peritectic reaction. Because the temperature of quasi-peritectic reaction is 140 °C [17], which is close to the eutectic temperature, the two reaction peaks tend to overlap, indicating that the Sn−52Bi−1.8Sb composition is close to the quasi-peritectic composition.

3.3 Wettability and interfacial structure of Sn−Bi−Sb/Cu

Resin flux and organic flux were used in the

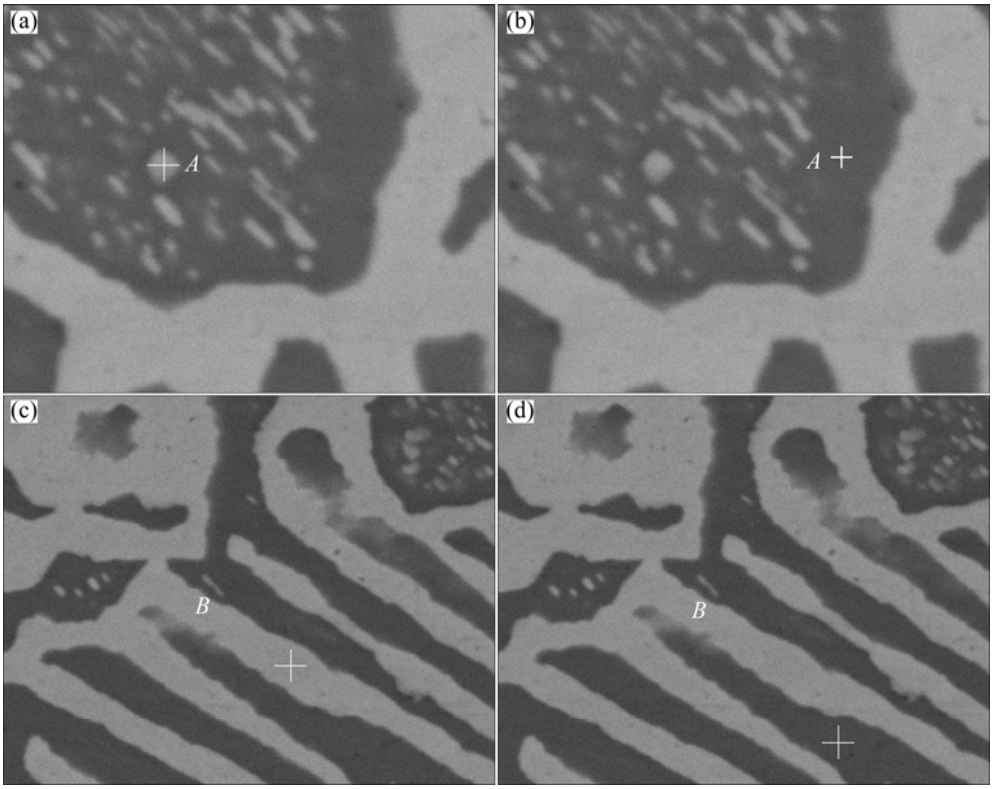

Fig. 3 EDX analysis of Sn−Bi−Sb alloy: (a) Light phase in part *A*; (b) Dark phase in part *A*; (c) Light phase in part *B*; (d) Dark phase in part *B*

Table 1 EDX analysis results of different phases in Fig. 3

Phase	Mass fraction/%		
	Sn	Bi	Sb
Light phase in part *A*	43.76	53.52	2.72
Dark phase in part *A*	85.88	12.99	1.13
Light phase in part *B*	2.16	96.72	1.12
Dark phase in part *B*	83.50	15.05	1.45

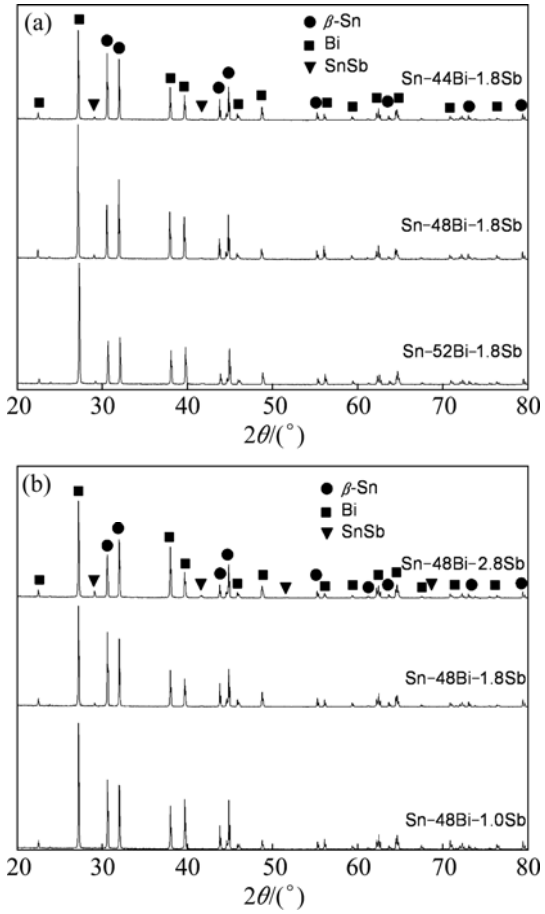

Fig. 4 XRD patterns of Sn−*x*Bi−1.8Sb (a) and Sn−48Bi−*x*Sb alloys (b)

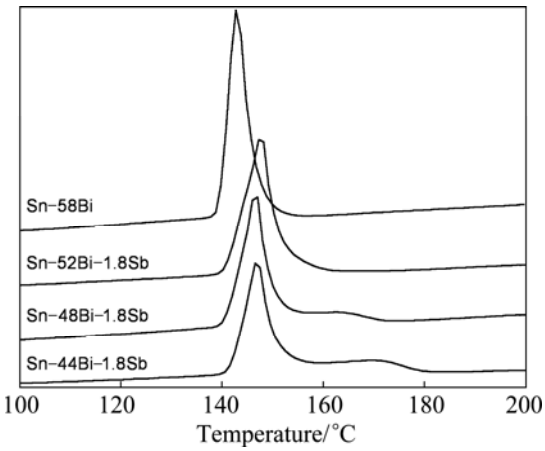

Fig. 5 DSC profiles for Sn−*x*Bi−1.8Sb alloys and Sn−58Bi alloy (on heating)

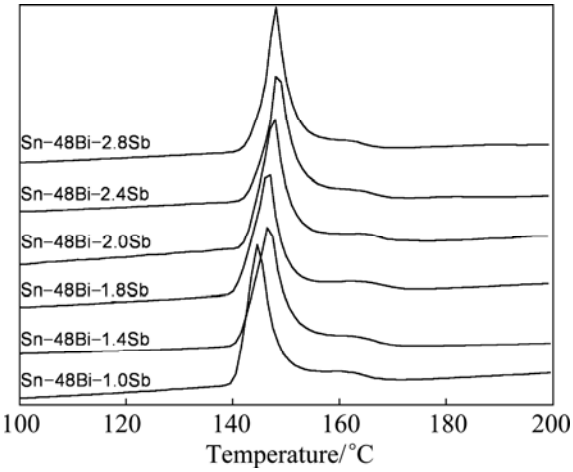

Fig. 6 DSC profiles for Sn−48Bi−*x*Sb alloys (on heating)

spreading test, respectively. Figure 7 shows the results of the spreading test. It is seen that when the Sb content is fixed, the highest spreading ratio reaches at Bi content of 48%. For the alloys with Sb content changing, the spreading ratio first increases and then drops, reaching the summit when Sb content is 2.0%. For all the Sn−Bi−Sb solders, the highest spreading ratio is 78.2%, which is higher than that of Sn−58Bi. The resin flux and organic flux show similar change with the variation of Bi and Sb contents, while organic flux behaves better.

The spreading ratio of Sn−Bi−Sb solders is affected by three factors, liquidus temperature, physical wetting and reactive wetting [18,19]. In this work, Bi mainly affects the wettability of Sn−Bi−Sb alloys on Cu substrate from two aspects. On one hand, increasing Bi can enhance the degree of overheating, as shown in Table 2, which favors the wetting. On the other hand, higher Bi, which means lower Sn, causes the reactive wetting to decrease. The decline of reactive wetting impedes the wettability. The results show that the spreading ratio changes a little when Bi content changes. Sb also affects the wettability from two aspects. Higher Sb accelerates the reactive wetting while the degree of overheating decreases. When the Sb content changes from 1.0% to 1.8%, the degree of overheating decreases and reactive wetting accelerates, which leads to the similar spreading ratio. As the Sb content continues to increase to 2.8%, the compounds generated from excessive reaction between solders and Cu block the solder to spread [20]. As a consequence, the optimum Sb content for wetting is about 2%.

When Sb is added into Sn−Bi solders, the interface structure between solder and Cu substrate changes. Figure 8 shows the microstructure and EPMA line analysis profiles of the Sn−Bi−Sb/Cu interface. There are only Cu and Sn across the diffusion reaction layer between Sn−58Bi and Cu, which suggests that Sn

Table 2 Reaction temperatures of Sn−*x*Bi−1.8Sb alloys and Sn−58Bi alloy

Alloy	Main peak temperature/°C	Second peak temperature/°C	Solidus temperature/°C	Liquidus temperature/°C	Melting range/°C
Sn−58Bi	143.1	−	139.4	148.0	8.6
Sn−52Bi−1.8Sb	147.7	−	140.6	152.0	11.4
Sn−48Bi−1.8Sb	146.5	163.0	140.9	172.7	31.8
Sn−44Bi−1.8Sb	146.9	169.0	141.9	180.5	38.6

Table 3 Reaction temperatures of Sn−48Bi−*x*Sb alloys

Alloy	Main peak temperature/°C	Second peak temperature/°C	Solidus temperature/°C	Liquidus temperature/°C	Melting range/°C
Sn−48Bi−1.0Sb	144.7	162.0	140.6	168.7	28.1
Sn−48Bi−1.4Sb	146.8	163.3	141.2	170.4	29.2
Sn−48Bi−1.8Sb	146.5	163.0	140.9	172.7	31.8
Sn−48Bi−2.0Sb	147.6	164.4	142.3	169.7	27.4
Sn−48Bi−2.4Sb	148.5	163.3	142.8	169.3	26.5
Sn−48Bi−2.8Sb	148.0	162.6	143.6	168.4	24.8

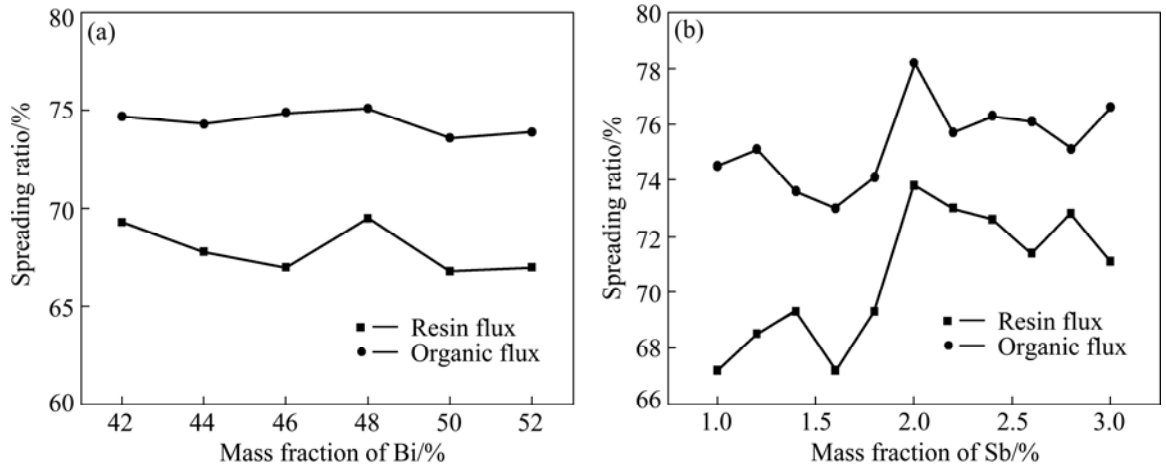

Fig. 7 Spreading ratios of Sn−*x*Bi−1.8Sb alloys (a) and Sn−48Bi−*x*Sb alloys (b) at 190 °C

diffuses preferentially. For ternary alloys, Sb is found in the diffusion reaction layer between Sn−Bi−Sb and Cu. The plateaus of Sn and Sb discovered in the diffusion reaction layer imply that Sb participates in the interface reaction. Table 4 shows the total thickness of the interfacial layers formed at the interface of the Sn−Bi−Sb/Cu joint. It can be seen that the total thickness of interfacial layers increases with the increase of Sb content.

3.4 Mechanical property and fracture morphology

The values of shear strength of Sn−Bi−Sb/Cu joints are shown in Table 5. It shows that when the Bi content decreases, the shear strength of the joints decreases. When the Sb content increases, the shear strength first changes a little and then increases obviously until the Sb content exceeds 2%. The shear strength of Sn−48Bi−2.4Sb is even higher than that of Sn−58Bi. Figure 9 shows the fractographs of Sn−Bi−Sb solders. All of the alloys display the ductile dimples. As the Bi content decreases and the Sb content increases, the alloys show more ductility. This may explain the drop of the shear strength of Sn−Bi−Sb alloys. Sb dissolves in the Sn and Bi matrix. The dissolution of Sb has two effects. One is solution strengthening. The other is to change the structure of solders, which leads to the segregation of Bi. When the Sb content reaches 2.4%, the proportion of eutectic structure resulting from quasi-peritectic reaction decreases obviously (Fig. 2(i)), which may contribute to the increase of shear strength.

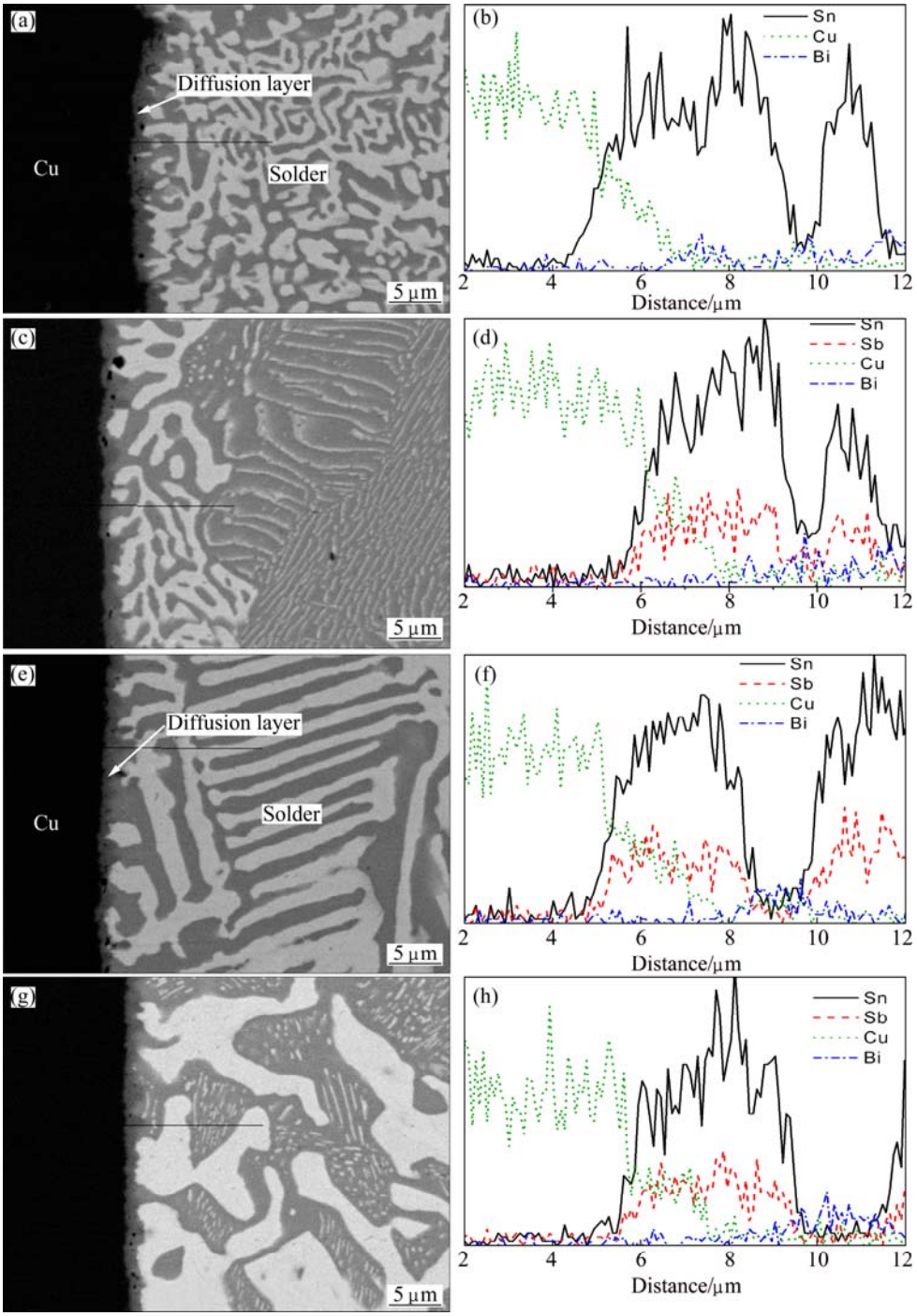

Fig. 8 SEM images (a, c, e, g) and EPMA analyses (b, d, f, h) of Sn−Bi−Sb/Cu joint: (a), (b) Sn−58Bi/Cu; (c), (d) Sn−48Bi−1.4Sb/Cu; (e), (f) Sn−48Bi−2.0Sb/Cu; (g), (h) Sn−48Bi−2.4Sb/Cu

Table 4 Total thickness of Sn−Bi−Sb/Cu reaction layers

Alloy	Layer thickness/μm
Sn−58Bi	2.34
Sn−52Bi−1.8Sb	2.43
Sn−48Bi−1.4Sb	2.43
Sn−48Bi−1.8Sb	2.51
Sn−48Bi−2.0Sb	2.76
Sn−48Bi−2.4Sb	2.85

Table 5 Shear strength of Sn−Bi−Sb/Cu joints

Alloy	Shear strength/MPa
Sn−58Bi	55.5
Sn−52Bi−1.8Sb	53.0
Sn−48Bi−1.4Sb	45.2
Sn−48Bi−1.8Sb	45.8
Sn−48Bi−2.0Sb	47.1
Sn−48Bi−2.4Sb	66.7

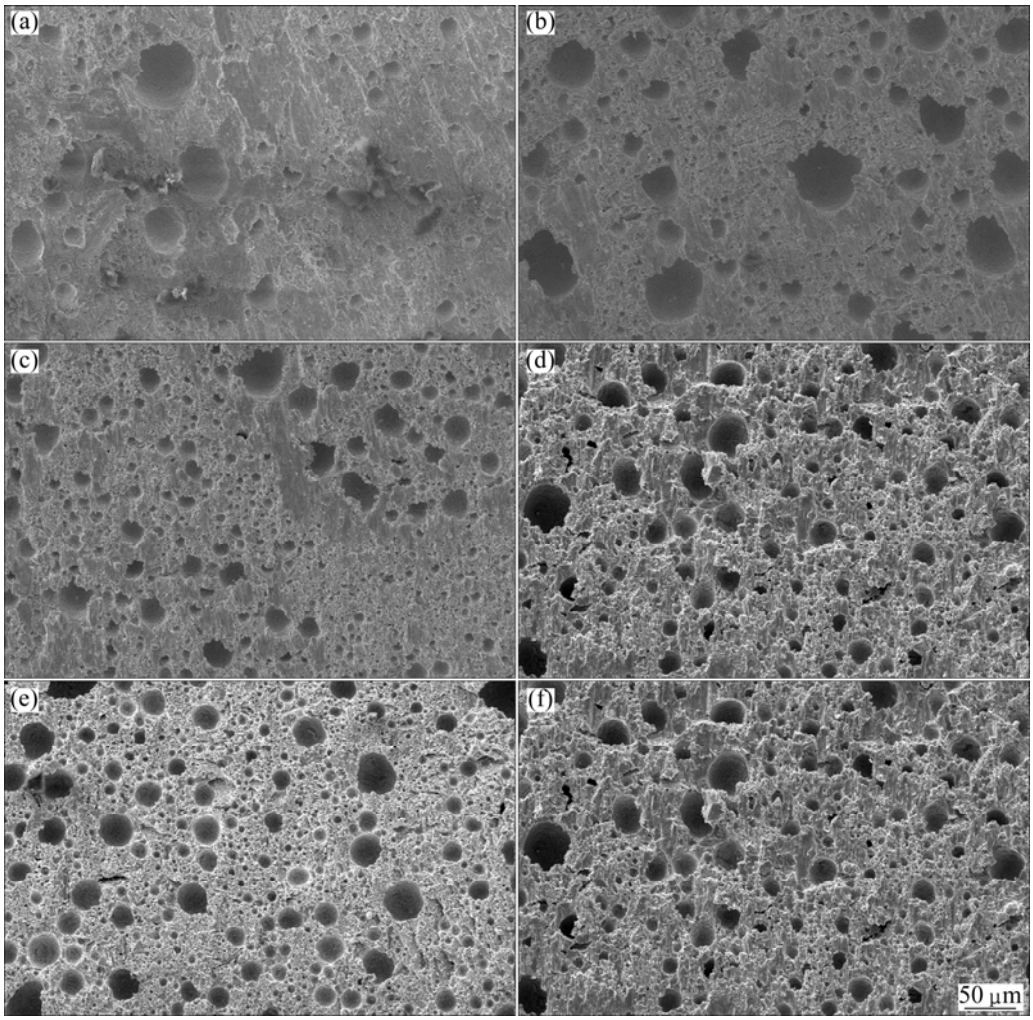

Fig. 9 Fracture morphologies of Sn−Bi−Sb/Cu joints: (a) Sn−58Bi; (b) Sn−52Bi−1.8Sb; (c) Sn−48Bi−1.4Sb; (d) Sn−48Bi−1.8Sb; (e) Sn−48Bi−2.0Sb; (f) Sn−48Bi−2.4Sb

4 Conclusions

1) The structure of Sn−Bi−Sb solders consists of Sn phase, Bi phase and SnSb intermediate phase. As Sb content increases, the SnSb intermediate phase increases.

2) As Bi content declines, the melting point and melting range become large. When the Sb content increases, the melting range and liquidus temperature increase first and then start to drop. The Sn−52Bi−1.8Sb composition is close to the quasi-peritectic composition.

3) The addition of Sb has an important effect on the spreading ratio of Sn−Bi−Sb alloy while Bi does not. Sn−48Bi−2Sb alloy possesses the highest spreading ratio. The IMC layer at Sn−Bi−Sb/ Cu interface consists of Cu, Sn and Sb. The layer becomes thick when the amount of Sb increases.

4) When Bi is fixed, increasing the Sb content can improve the shear strength of the joints, especially when the Sb content exceeds 2%.

References

[1] ZHANG Shu-guang, HE Li-jun, ZHANG Shao-ming, SHI Li-kai. Progress of research and application of lead-free solder [J]. Materials Review, 2004, 18(6): 72−75.

[2] ARRA M, SHANGGUAN D, YI S, THALHAMMER R, FOCKENBERGER H. Development of lead-free wave soldering process [J]. IEEE Transactions on Electronics Packaging Manufacturing, 2002, 4: 289−299.

[3] MA Ju-sheng. Lead-free solder materials for sustainable development of green electronics [C]//Proceedings of the 6th International Conference on Electronics Packaging Technology. Shenzhen, 2005: 45−51.

[4] MULUGETA A, GUNA S. Lead-free solders in microelectronics [J]. Materials Science and Engineering R, 2000, 27: 95−141.

[5] BAR-COHEN A, KRAUS A D, DAVIDSON S F. Thermal frontiers in the design and packaging microelectronic equipment [J]. Mechanical Engineering, 1983, 105(6): 53−59.

[6] HWANG J S. Environment-friendly electronics: Lead-free technology [M]. Isle of Man: Electrochemical Publication Ltd, 2001.

[7] BRAGA M H, VIZDAL J, KROUPA A, FERREIRA J, SOARES D, MALHEIROS L F. The experimental study of the Bi−Sn, Bi−Zn and

Bi−Sn−Zn systems [J]. Computer Coupling of Phase Diagrams and Thermochemistry, 2007, 31: 468−478.
[8] HU Li, ZENG Ming, SHEN Bao-luo. Research of Sn−Bi lead-free solder [J]. Modern Electronics Technique, 2009, 32(16): 164−167.
[9] ZOU H F, ZHANG Q K, ZHANG Z F. Eliminating interfacial segregation and embrittlement of bismuth in SnBi/Cu joint by alloying Cu substrate [J]. Scripta Materialia, 2009, 61(3): 308−311.
[10] MEI Z, MORRIS J W. Characterization of eutectic Sn−Bi solder joints [J]. Journal of Electronic Materials, 1992, 21(6): 599−607.
[11] MORRIS J W, GOLDSTEIN J L, MEI Z. Microstructure and mechanical properties of Sn−In and Sn−Bi solders [J]. Journal of Electronic Materials, 1993, 7: 25−27.
[12] ZHU Q S, ZHANG Z F, WANG Z G, SHANG J K. Inhibition of interfacial embrittlement at SnBi/Cu single crystal by electrodeposited Ag film [J]. Journal of Material Research, 2008, 23(1): 78−82.
[13] LI Yuan-shan, CHEN Zhen-hua, LEI Xiao-juan. Influence of rapid cooling and diffusion annealing on Sn−Bi−X solder [J]. The Chinese Journal of Nonferrous Metals, 2007, 17(8): 1319−1324. (in Chinese)
[14] MANASIJEVIC D, VRESTAL J, MINIC D, KROUPA A, ZIVKOVIC D, ZIVKOVIC Z. Phase equilibria and thermodynamics of the Bi−Sb−Sn ternary system [J]. Journal of Alloys and Compounds, 2007, 438: 150−157.
[15] WANG C Q, LI M Y, TIAN Y H, KONG L C. Review of JIS Z 3198: Test method for lead-free solders [J]. Electronics Process Technology, 2004, 3: 47−54.
[16] GHOSH G, LOOMANS M, FINE M E. An investigation of phase equilibria of the Bi−Sb−Sn system [J]. Journal of Electronic Materials, 1994, 23(7): 619−623.
[17] OHTANI H, ISHIDA K. Thermodynamic study of the phase equilibria in the Bi−Sn−Sb system [J]. Journal of Electronic Materials, 1994, 23(8): 747−755.
[18] YOST F G, SACKINGER P A, OTOOLE E J. Energetics and kinetics of dissolutive wetting processes [J]. Acta Mater, 1998, 46(7): 2329−2336.
[19] YOST F G. Kinetic of reactive wetting [J]. Scripta Materialia, 2000, 42: 801−806.
[20] PAVEL P, ANNE T, VLADIMIR T, NICOLAS E. The role of intermetallics in wetting in metallic systems [J]. Scripta Materialia, 2001, 45: 1439−1445.

Sb 含量对 Sn−Bi 系焊料性能的影响

张 成[1]，刘思栋[1]，钱国统[2]，周 健[1]，薛 烽[1]

1. 东南大学 材料科学与工程学院，南京 211189；
2. 绍兴市天龙锡材有限公司，绍兴 312001

摘 要：研究 Sb 元素含量对 Sn−Bi 系焊料性能的影响。通过差示扫描量热法研究 Sn−Bi−Sb 焊料的熔化行为。采用铺展实验研究焊料在 Cu 基板上的润湿性。测试 Sn−Bi−Sb/Cu 结合界面的力学性能。结果表明：三元合金中含有包共晶反应形成的共晶组织，随着 Sb 含量的增加，共晶组织增多；在加热速率为 5 °C/min 的条件下，三元合金显示出更高的熔点和更宽的熔程；添加少量 Sb 对 Sb−Bi 系焊料的铺展率有影响；在焊料铺展过程中形成反应过渡层，反应过渡层中存在 Sb 元素而无 Bi 元素，过渡层厚度随着 Sb 元素含量的增加而增大。Sn−Bi−Sb 焊料的剪切强度随着 Sb 元素含量的增加而升高。

关键词：无铅焊料；Sn−Bi−Sb 合金；显微组织；熔化行为；润湿性

(Edited by Wei-ping CHEN)